

APPLICATION OF LE-FDTD ANALYSIS TO NON-LINEAR CIRCUITS, INCLUDING GaAs DEVICES

G. Stopponi, L. Roselli, and P. Ciampolini

Istituto di Elettronica, Università di Perugia, Via G. Duranti, 1/A-1, 06131 Perugia, Italy

Abstract

We discuss the application of the Lumped-Element, Finite-Difference Time-Domain (LE-FDTD) algorithm to the analysis of a planar active antenna. Through this approach, the full-wave signal propagation along the passive network is taken into account, at the same time accounting for non linear devices to be comprehensively considered. GaAs, as well as silicon, devices can be self-consistently taken into account, and described either by a compact, analytical equations set, or by a distributed, numerical solution of the semiconductor transport equations. Both approaches are illustrated in the paper: a GaAs Gunn diode is used to excite a slot antenna, and is modeled at the distributed level; the same structure is then used as a frequency multiplier: in this case, non linearity is introduced by a Schottky diode, which is described by a compact equivalent circuit. In both cases, influence of the diode placement across the slot is briefly discussed.

1. Introduction

Numerical modeling of non-linear circuits represents a indispensable aid for the fast and efficient design of advanced microwave and millimeter-wave circuits: several CAD options are actually available to the designer, ranging over a wide range of features.

Established commercial packages exploit conventional circuit-analysis techniques, extended to the microwave range by introducing sophisticated equivalent networks for the circuit components (active, as well as passive). Such an approach attains a high grade of computational efficiency and versatility. However, when complex geometries come into play, or when strong coupling among circuit components (and/or package) occurs, tuning of the equivalent network becomes critical. More generally, equivalent-circuit representation is intrinsically little suitable for the description of radiative propagation effects. To overcome this bottleneck, the inherent distributed nature of such phenomena can be accounted for by the full-wave analysis of electromagnetic field propagation. Several strategies have been pursued to achieve this goal: in the following, we shall refer to the Finite-Difference, Time-Domain (FDTD) method, firstly introduced by Yee [1] for the solution of Maxwell's equations, extended to account for lumped, non-linear devices according to the treatment devised by Sui *et al* [2].

We have developed a 3D Maxwell solver based on the Lumped-Element, Finite-Difference Time-Domain (LE-FDTD) scheme, and have extended such an approach to incorporate distributed, as well as lumped device models. More specifically, although the lumped device assumption is actually retained (i.e., no account for E.M. propagation is given within the device), numerical device simulation techniques are exploited to describe the active components behavior. This, at the expense of increased computational demand, makes it unnecessary the formulation of a device compact (i.e., Spice) model, and, mostly relevant, reduces at a minimum the need of parameters characterization. It therefore can be especially useful for circuits including somehow non-conventional devices and, in particular, for MMIC devices, where a close link between the fabrication process details and the circuit performance can be exploited for optimization purposes.

In Sect. 2 below, fundamentals of the method are reviewed, whereas a set of applications is illustrated in Sect. 3. Here, a simple slot structure is used to obtain both an active antenna and a frequency multiplier. To provide excitation of the antenna, the negative differential resistance provided by a Gunn device is exploited; to carefully describe the dynamic behavior of such a device, distributed, device-level modeling has been used in this case. A more conventional Schottky diode has been used to introduce the multiplier non-linearity: in this case, a compact device model has been used instead. Eventually conclusions are drawn in Sect. 4.

2. The LE-FDTD algorithm

Standard FDTD techniques are adopted for the solution of the Maxwell's equation: field components are mapped on the edge of a 3D, orthogonal, variable-size mesh. Extension to active, non linear components is carried out under the assumption of negligible device size, with respect to the signal wavelength; this implies the device active-size being smaller than the spatial discretization step, so that a lumped bipole can be connected to a single mesh cell, as shown in Fig. 1. This results in an additional current contribution \vec{J}_{cl} , showing up in the Maxwell's curl-II equation:

$$(1) \quad \nabla \times \vec{H} = \epsilon \frac{d\vec{E}}{dt} + \vec{J}_{cd} + \vec{J}_{cl}$$

and summing to the current density flowing along the distributed media \vec{J}_{cd} . Such a current contribution comes from the solution of the lumped device equations; in the simplest case, a set of analytical equations, which describe the device transient behavior (including reactive components) is solved. If a more accurate solution is required (or if no suitable device model is at hand), such a current can be extracted from the distributed solution of the semiconductor transport equations: at present, a 1D, drift-diffusion solver has been incorporated to test the method; in principle, the extension to multidimensional or more sophisticated transport models poses little problems. In both cases, non-linear solution is obtained through an iterative (Newton-Raphson) procedure: a solution algorithm has been devised, which, although preserving self-consistency, avoids full coupling of device and field equations. This algorithm represents an extension of the "leapfrog" scheme typical of FDTD solvers, and requires no iterated solution of Maxwell's equation over the whole passive domain. According to such a scheme, equation coupling occurs on a strictly local basis: details on the interfacing procedure are given in [3]. Here, we shall only briefly comment on the extension to GaAs, distributed device models, obtained by introducing within the constitutive equations of the semiconductor transport model the empirical, field-dependent electron-mobility model recalled below [4]:

$$(2) \quad \mu_n(E) = \frac{\mu_o + v_{sat} \cdot E^3/E_o^4}{1 + (E/E_o)^4}$$

The expression above has been discretized and incorporated into the mixed-mode simulation code, thus making it suitable for the physical simulation of the Gunn oscillator described in the next section.

3. Simulation examples

The structure shown in Fig. 2 has been selected to exemplify the simulation code features: it consists of a $5.66 \times 0.4 \text{ mm}^2$ aperture on a single-side, copper plates insulating substrate. The active device bias is provided by a coplanar waveguide, inserting at a slot edge. This can be regarded as an elementary cell of an array structure, and has been conceived as a scaled-down prototype of a device compatible with MMIC-technology. As introduced before, the same passive structure has been completed by different active devices, in order to highlight different functionalities: a frequency multiplier is obtained by inserting a Schottky diode across the aperture, whereas, by inserting a Gunn device, self-oscillation can be triggered, recovering the behavior of an active antenna.

To analyze the frequency multiplier, the circuit has been illuminated by a planar wave at 10.5 GHz frequency, corresponding to the first resonant mode of the passive structure. The Schottky diode is described by the analytical model introduced in [5], and, at the frequency above, features a 50Ω impedance.

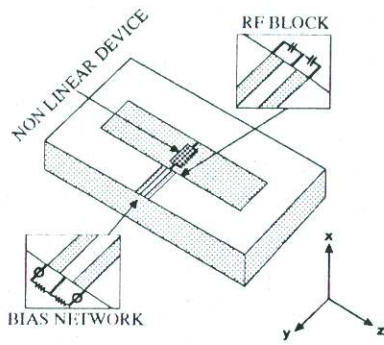


Fig. 2: sketch of the simulated structure.

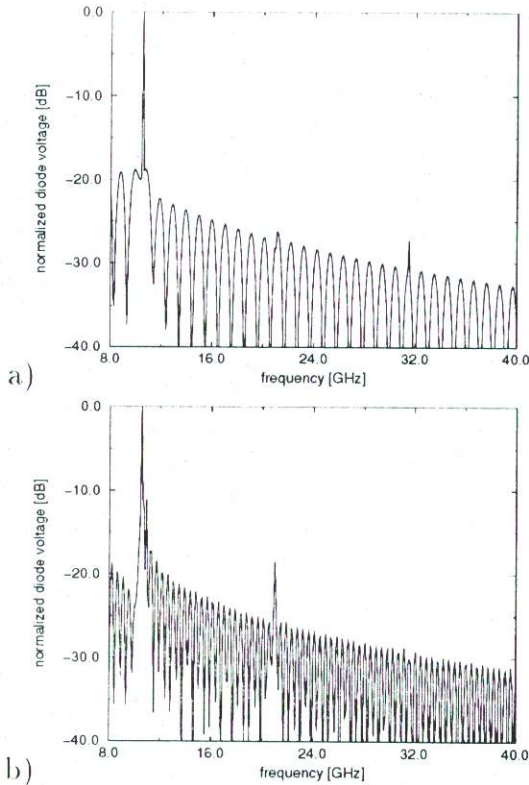


Fig. 3: Frequency multiplier spectra, for diode placed at mid-slot (a), and close to the slot's end (b).

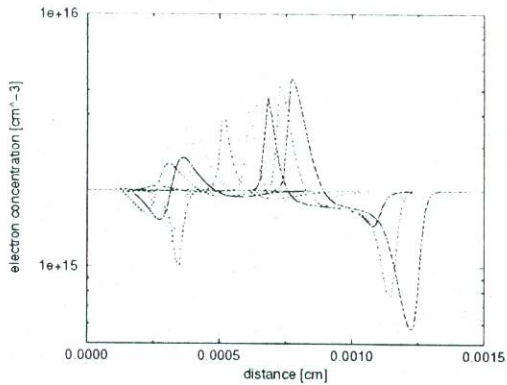


Fig. 4: Electron concentration profile within the Gunn diode, at 11 ps time intervals.

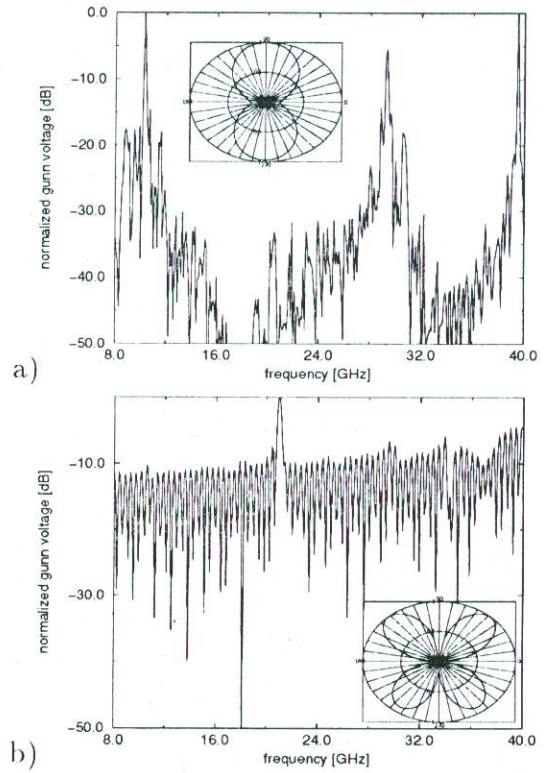


Fig. 5: Gunn-diode active antenna spectra, for diode placed at mid-slot (a), and close to the slot's end (b).

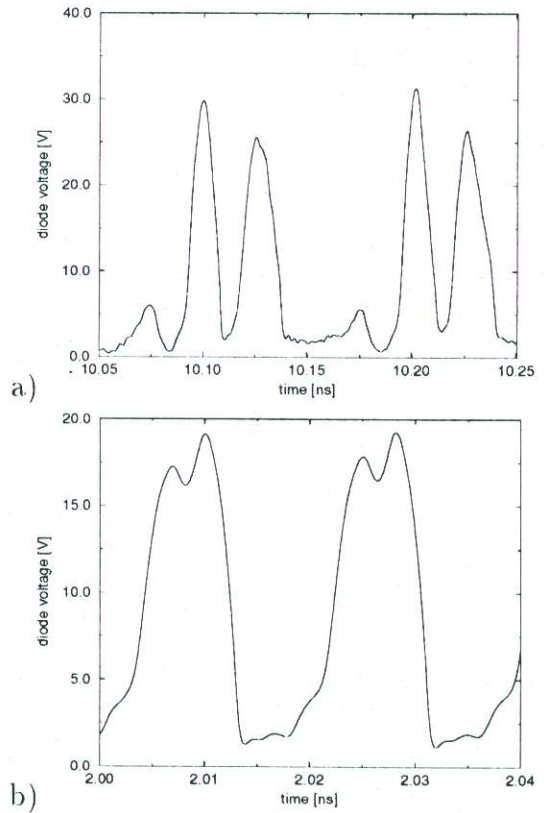


Fig. 6: Gunn-diode voltage waveform, for diode placed at mid-slot (a), and close to the slot's end (b).